2024 European Control Conference (ECC)
June 25-28, 2024. Stockholm, Sweden

Bio-Inspired Adaptive Fuzzy Control Systems for Precise Low-Altitude Hovering of an Unmanned Aerial Vehicle Under Large Uncertainties

Fendy Santoso[1,2], Matthew A. Garratt[2], Sreenatha G. Anavatti[2], Jiefei Wang[2],
Phi Vu Tran[2], and M. Meftahul Ferdaus[3]

[1] *Artificial Intelligence and Cyber Futures Institute, Charles Sturt University, Canberra, ACT 2600, Australia*
[2] *School of Engineering and Technology, University of New South Wales Canberra, Campbell, ACT 2612, Australia*
[3] *Department of Computer Science, University of New Orleans, New Orleans, LA 70148, United States*
Corresponding Author: fsantoso@csu.edu.au

***Abstract*—The ability to learn and adapt to unknown system dynamics simplifies controller design and enables complex platforms to be controlled without the need to build complex mathematical models. Taking some inspiration from *the way humans learn*, we present the concept of bio-inspired self-learning in aerial robotics, leveraging on the concept of an adaptive Takagi-Sugeno (TS)-fuzzy control system. The main distinguishing feature of the evolving TS-fuzzy system is the ability to learn from scratch, eliminating the need to have *a-priori* knowledge about the system as in the traditional model-based control systems. Besides, the system can also learn from certain predefined rules. As opposed to traditional fuzzy systems, which require *prior* training (knowledge) to build their structure, the evolving TS-fuzzy system needs no such *prior* knowledge since the controller can perform online self-learning. Also, its ability to capture high-degree of uncertainties (e.g. severe ground effects due to low-altitude flying) is very advantageous. To demonstrate the efficacy of the control systems, we design and implement the evolving TS-fuzzy autopilots in the five control loops of our Tarot hexacopter drone after conducting extensive computer simulations using non-linear aerodynamics models. We also compare the efficacy of the autopilot systems with respect to the effectiveness of traditional PID controllers in the altitude control loop as a benchmark.**

***Index Terms*—Adaptive Control, Bio-Inspired Self-Learning, Takagi-Sugeno (TS) Fuzzy Systems, Unmanned Aerial Vehicle**

I. Introduction

Adaptive and intelligent control systems have received considerable attention in the past few years [1], [2]. They refer to a class of control systems that can dynamically adjust their behaviors via their adaptive control laws in response to the varying dynamics of the plants or flight environments (e.g. due to uncertainties and disturbances). Thus, adaptive control systems differ from their fixed-gain counterparts because of their adaptation mechanisms, which are mainly calculated based on the current and the previous measurements of the dynamics of the systems [3].

This research was supported by the Defence Science and Technology (DST) Group Australia through the DST Competitive Evaluation Research Agreement (CERA) program. The title of the project was CERA 259: Feasibility Testing for Adaptive Flight Control of a Dragonfly-Inspired Micro Air Vehicle. In particular, we would like to thank Dr. Jia Kok from the DSTG, Australia, who has worked with us to develop the program objectives.

Fig. 1. Our experimental hexacopter unmanned aerial vehicle hovers at low-altitude subjects to severe ground effects. The system employs the Intel Edison computer on-module as its main information processing system. The MAVLink (Micro Air Vehicle communication) protocol interfaces the system to the PixHawk2 Flight Controller Unit (FCU) and the flight stack. Our system has a challenging payload configuration (up to 10 kg take-off weight).

For this reason, adaptive control can be more tolerant to uncertainties and varying operating points in the system characteristics and signal models compared to fixed-gain controllers, which are entirely designed under the assumptions of fixed system models (dynamics). Unless sufficiently robust, the performance of fixed-gain controllers may gradually degrade over time as the characteristics of the system evolve.

Owing to the advancements in soft computing and machine learning, many researchers have envisioned the concept of intelligent machines, namely, machines that can learn or be trained independently with minimum human interventions. Although the concept of the evolving fuzzy algorithms (structural and parametric adaptive system) has been around for some time [1], the real-time implementations of those algorithms, especially, in aerial robotics were hampered by the computational capability of the onboard autopilot. Thus, many researchers still heavily focus on the use of traditional control approaches.

To date, most people still employ model-based control systems. For instance, Chen et al. in [4] introduced a sliding mode-based control system, Lee et al. in [5] introduced feedback linearization-based trajectory tracking, Pokswa et al. in [6] developed gain scheduling attitude control of a fixed-wing UAV with automatic controller tuning.

In the aforementioned techniques, the efficacy of the control systems is reliant on the availability of accurate mathematical models, which in many cases are not directly or practically available. Also, there is no perfect mathematical model in real life. Despite their past historical success, the process of applying gain scheduling control is quite tedious due to the requirement to have multiple linearized models over the flight envelope of an aircraft as a result of the time-varying nature of the system, namely, different conditions of operating points, such as varying velocities and altitudes, exacerbated with uncertainties and non-linearities in the assumed mathematical models.

The advantages of fuzzy systems over conventional control systems have been established beyond doubt. Designed based on human intuition and optimized based on data sets or data flows, fuzzy systems are more straightforward from the perspective of laypersons (e.g. ordinary drone operators) [1]. Model-free fuzzy systems are more efficient and robust ([7]) compared to conventional control theory ([8], [9]), whose performance relies on the accuracy of the assumed mathematical models of the systems.

Research on intelligent algorithms encompasses a wide spectrum of scientific disciplines, such as guidance (path-planning) systems [10], [11], [12] as well as adaptive and learning control for unmanned vehicles, such as the concept of differential evolution [13] to optimize the performance of the onboard PID controller of a quadrotor aircraft. Although some researchers have designed learning autopilots using neural networks (e.g. [14]) and fuzzy logic autopilots; [15]; to the best of our knowledge, the benefits of the *evolving* Takagi-Sugeno (ETS) fuzzy systems to facilitate real-time and direct *self-learning* in aerial robotics have not been discussed in the literature.

This research gap has motivated us to investigate the efficacy of the evolving TS-fuzzy systems in a fast dynamic system, such as in our hexacopter platform as in Fig. 1. Consequently, our research contributions are as follows:

1) We propose the concept of the bio-inspired flying robot by designing and simultaneously implementing five evolving TS-fuzzy-based control loops (roll, pitch, and the coordinate positions across the (x, y, z)-axes, namely, p_x, p_y, and p_z) in our Tarot hexacopter and test the performance in the real-time flight tests. We believe our work is the *first* in the literature that advocates the concept of learning from scratch by applying the evolving TS-fuzzy system in a fast dynamic aerial robotic platform, that is, to achieve a stable low-altitude hovering for a hexacopter drone in the face of significant uncertainties.
2) For analysis, we employ high-fidelity *non-linear* aerodynamics models as we approach the dynamics of our hexacopter using the blade momentum theory, suitable for multi-rotor vehicles. Unlike many studies neglecting the cross-coupling behaviors of the system (e.g. [16], [17]); we take into account the cross-coupling dynamics of our hexacopter platform by modeling their behaviors from the real-time flight data.
3) We conduct a rigorous comparative study regarding the efficacy of our fuzzy control systems relative to the performance of the traditional PID controllers in real-time flight tests for low-altitude hovering, where the system is constantly faced with severe ground effects.

It should be highlighted that the word 'bio-inspiration' is due to the nature of the bio-inspired learning process itself, mimicking *the human way of learning*, such as adding important rules (i.e. managing knowledge) while updating the existing rules as necessary as the system constantly receives new information from the sensors. This process is analogous to the way we learn in our day-to-day lives while imitating the concept of natural evolution i.e. the survival of the fittest. In fact, our knowledge evolves every day as we experience new things in life. We tend to forget unused or unimportant past knowledge while updating, upgrading, and adding relevant knowledge based on the daily information received. This is where the term 'bio-inspired' comes into the picture.

The remainder of this manuscript is organized as follows. While Section II highlights the hardware configuration of our system, Section III discusses the non-linear rigid body dynamics from the first principle. Meanwhile, Section IV elaborates on the architecture of our fuzzy control system. Section V presents extensive computer simulations to highlight the efficacy of our autopilots. Section VI presents the real-time performance of our closed-loop flight control systems. Section VII concludes this paper.

II. Hardware Configuration

Built from a kit, we employ a commercial Tarot 680-Pro hexacopter drone as indicated in Fig. 1. The reason to employ this aerial platform is due to its robustness. The drone has a maximum take-off weight of 10 kg and it is able to endure of a maximum 15 minutes of flight time. Considering its autopilot system, we employ hierarchical double loop control systems, meaning the attitudes (e.g. pitch (longitudinal), roll (lateral), and yaw (directional)) are controlled in the inner loop, while the coordinate positions are regulated in the outer loop.

Owing to its benefits, namely, compact size, low power consumption, and compatibility with PixHawk2 autopilot, we select the Intel Edison (a dual-core Intel Atom 500 MHz x86 microprocessor) as its computer-on-module of our drone. The system is supported with a DRR400 memory of 1 GB, an EMMC onboard memory of 4 GB, and a WiFi communication network. Considering the MAVLink protocol, the Edison will be interfaced with the Pixhawk2 Flight Controller Unit (FCU) and flight stack. Under the MAVROS extendable communication node for Robot Operating System (ROS) supported by a proxy for ground station control, the system employs an asynchronous serial connection at 921,600 bauds to facilitate data communication between the Pixhawk2 autopilot and the Intel Edison systems.

III. Non-Linear Rigid Body Dynamics of Our Hexacopter Unmanned Aerial Vehicle

The dynamics of our drone can be represented using the following state variables i.e., $[x\ y\ z\ \dot{x}\ \dot{y}\ \dot{z}\ \phi\ \theta\ \psi\ \dot{\phi}\ \dot{\theta}\ \dot{\psi}]^T$, in which $(x,\ y,\ z)$ denotes the body coordinates, namely, the positions of the aerial vehicle with respect to the global coordinate system, $(\dot{x},\ \dot{y},\ \dot{z})$ point outs the linear velocities along the (x, y, z) axes while $(\phi,\ \theta,\ \psi)$ highlights the orientations of the aerial vehicle, namely, roll, pitch, and yaw angles, respectively. Moreover, $(\dot{\phi},\ \dot{\theta},\ \dot{\psi})$ represents the angular velocities of the system.

We treat our drone as a rigid body to study its dynamics. Considering the second law of Newton applied on a rotating body frame with an angular velocity ω, the total translational forces $\sum \vec{F}$ acting on a rigid body with a mass m and the linear velocity v can be described as follows:

$$\sum \vec{F} = m\frac{d\vec{v}}{dt}\bigg|_I = m\frac{d\vec{v}}{dt}\bigg|_B + m(\vec{\omega} \times \vec{v}). \tag{1}$$

Considering (1), the derivation of the rigid body translational dynamics of an aerial vehicle can be obtained as follows [18]:

$$\begin{cases} \sum F_x = m(\dot{u} + qw - rv) = X - mg\sin\theta \\ \sum F_y = m(\dot{v} + ru - pw) = Y + mg\cos\theta\sin\phi \\ \sum F_z = m(\dot{w} + pv - qu) = Z + mg\cos\theta\cos\phi \end{cases} \tag{2}$$

where m denotes the total mass of the aerial vehicle, $[\phi\ \theta\ \psi]^T$ indicates the attitudes of the system (roll, pitch, and yaw), $[u\ v\ w]^T$ is the linear velocity matrix along the $(x,\ y,\ z)$ axes, $\sum F_x\ , \sum F_y, \sum F_z$ indicate the total forces about the (x, y, z)-axes, $[X\ Y\ Z]^T$ presents the directional forces along the (x, y, z) axes, while $[p\ q\ r]^T$ denotes the rotational rates.

The equations for the rotational motions can be obtained in a similar fashion using the relation between the torque T and the angular momentum (momentum of momentum) H as follows:

$$\sum \vec{T} = \frac{d\vec{H}}{dt}\bigg|_I = \frac{d\vec{H}}{dt}\bigg|_B + (\vec{\omega} \times \vec{H}) \tag{3}$$

From (3), the moment equations, describing the rotational dynamics of a rigid body, by assuming that the product of Inertia $(I_{yz} = I_{xy} = 0)$, can be derived as follows [18]:

$$\begin{cases} L = I_x\dot{p} - I_{xz}\dot{r} + qr(I_z - I_y) - I_{xz}pq \\ M = I_y\dot{q} + rp(I_x - I_z) + I_{xz}(p^2 - r^2) \\ N = -I_{xz}\dot{p} + I_z\dot{r} + pq(I_y - I_x) + I_{xz}qr \end{cases} \tag{4}$$

where $[L\ \ M\ \ N]^T$ indicates the net torque to the rate of change of angular momentum; $I_x,\ I_y,\ I_z$ indicate the moments about the $(x,\ y,\ z)$-axes, and I_{xz} denotes the product of inertia. From (2) and (4), both the translational and rotational dynamics of an aerial vehicle can be described by six ordinary differential equations, which are coupled, and non-linear.

It should be noted that the ground effect is an undesirable phenomenon that usually comes into the picture in a hover flight when the altitude of the rotorcraft is less than three times the radius of the rotor of the system [19]. This is because the airflow pattern is significantly altered due to a physical obstruction introduced by the ground. Thus, the downwash velocity induced by the rotor will decrease, leading to a cushioning effect. As a result of the vertical lift for the same control input and power setting increases, which will also significantly introduce substantial non-linearity in our system. Ground effects can significantly alter the relationship between thrust and control inputs by up to 50 %, increasing the non-linearity of the system [20].

IV. Control System Architecture

The architecture of our hierarchical intelligent autopilot system is given in Fig. 2. We employ a mixing arrangement to convert the attitude and thrust commands from the controller to the speed of the motor. The ‘forces and moments’ block computes the thrust and torque of each rotor based on the relative airflow acting on each rotor and the commanded motor speed.

A. Online Learning of the Evolving TS-fuzzy Systems

We recall the concept of the online ETS algorithm as discussed in [21] as the basis of our fuzzy system. The step-by-step procedures for online learning in the ETS algorithm can be elaborated as follows. The system will initialize the antecedent part of the rules as it is initially set to have one rule only. Based on the arrival of data streams, the potential of each data sample will be recursively calculated The term potential $P_k(.)$ indicates the ability of a new data point to be a cluster center.

The potential of new data with respect to the potential of the existing focal points is used to modify or update the fuzzy rule-based structure, that is,

1) **IF** $P_k(z_k) > P_K(z_i^*),\ i = [1, 2, .., R],\ P_k(.)$ denotes the potential of a new data point and $P_K(z_i^*)$ indicates the potential of all existing centers **AND** the new data is closer to the old center, **THEN** a new center will be replaced by that particular data point, and
2) The system will add the rule based on the projection of a new center, to satisfy equation (5) as follows:

$$\frac{P_k(Z_k)}{\max_{k=1}^{R}\ P_k(z_i^*)} - \frac{\delta_{min}}{r} \geq 1, \tag{5}$$

$r \in [0.3\ 0.5]$ denotes a positive constant, indicating the spread of the antecedent and the zone of the influence of the ith model, that is, the radius of the neighborhood of a data point, and x_i^* denotes the focal point of the ith rule antecedent, and R is the number of rules.
3) Subsequently, we perform a recursive calculation of the new center and the parameters of the consequent functions by RLS (6) and (7). In this step, we estimate the local parameters using the weighted recursive least square (WRLS) technique as follows:

$$\hat{\pi}_{ik} = \hat{\pi}_{ik-1} + c_{ik}x_{ek-1}\lambda_i(x_{k-1})(y_k - x_{ek-1}^T\hat{\pi}_{ik-1}), k = 2, 3, ... \tag{6}$$

in which,

$$c_{ik} = c_{ik-1} - \frac{\lambda_i(x_{k-1})c_{ik-1}x_{ek-1}x_{ek-1}^T c_{ik-1}}{1 + \lambda_i(x_{k-1})x_{ek-1}^T c_{ik-1}x_{ek-1}}\ i = [1\ R] \tag{7}$$

The initial condition of the system is defined as $\hat{\pi} = 0$ and $c_{i1} = \Omega I$, where Ω is a large positive constant.

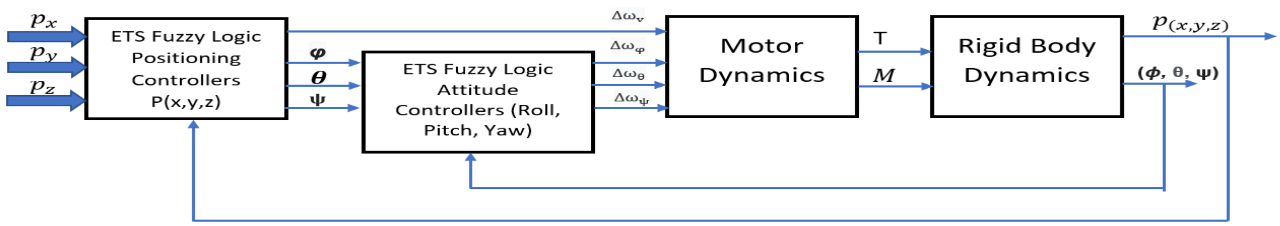

Fig. 2. The hierarchical ETS-fuzzy control system in our hexacopter. Inside the ETS block, the signal can be split into three types, namely, $e(t)$, $\dot{e}(t)$, and $\int e(t)dt$, mimicking the dynamics of the conventional PID controller. $\Delta\omega_{\{\phi,\theta,\psi\}}$ denote the rate of change of the speed of the motor (rotor) in response to the attitudes (roll, pitch, yaw) of the aerial vehicle. We employ a sampling frequency $f_s = 100$ Hz (T_s=0.01s).

4) Lastly, we calculate the subsequent output, that is, the output of the fuzzy system for the subsequent sampling time, determined by the online prediction as in (8), (9).

$$\hat{y}_{k+1} = \psi_k^T \hat{\theta}_k, \;\; k = 2, 3, ... \tag{8}$$

in which the system parameters $\hat{\theta}_k$ can be determined using the following Kalman filtering procedure:

$$\hat{\theta}_k = \hat{\theta}_{k-1} + C_k \psi_{k-1}(y_k - \psi_{k-1}^T \hat{\theta}_{k-1}), \;\; k = 2, 3, ..., \tag{9}$$

where $\psi_k = [\lambda_1(x_k)x_{ek}^T \lambda_2(x_k)x_{ek}^T ... \lambda_R(x_k)x_{ek}^T]^T$. To achieve a more informative and more compact system, we employ cluster potential, instead of distance. This is because the system takes into account the spatial information and the history of the data when adapting the fuzzy parameters associated with a certain rule while modifying the rule base structure [21]. Interested readers may also refer to [21] for details of the algorithm.

V. Computer Simulations

We conduct extensive numerical simulations to indicate the effectiveness of the proposed adaptive control system. We use the concept of *Hardware-in-The-Loop* (HIL) testing in our online simulations under the *Matlab C Mex S-function* environment. We explore the ability of the ETS controller to learn from scratch while stabilizing the dynamics of our hexacopter platform in its three control loops, namely, vertical, lateral, and longitudinal. Despite the model-free nature of the control systems; in our study, we also conduct numerical simulations. For this reason, we employ the high-fidelity non-linear mathematical models of aerial vehicles as also discussed in (1)-(4).

A. The Vertical Control Loop

The effectiveness of our autopilot systems in the vertical control loop is highlighted in Fig. 3, where we applied a unit step position reference signal with $z = 1m$ at $t = 1s$. In other words, the hexacopter was set to climb up vertically in the z-axis to reach its desired altitude. As can be seen, with the evolution of the control system, our hexacopter drone was successfully stabilized within a short period. Meanwhile, the evidence of learning of the ETS control system in the vertical loop is presented in Fig. 3. Fig. 3b represents the values of the cluster potential P_k against its upper and lower bounds limits P_{max} and P_{min}. As can be seen from Fig. 3a, during

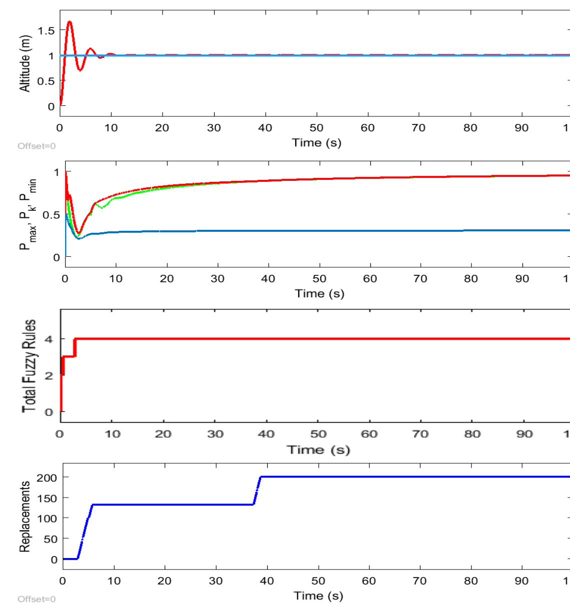

Fig. 3. The performance of our ETS controller in the vertical loop with respect to a constant altitude reference signal: (a) *Top figure*: Step response of the evolving TS controller for the vertical loop. While red line indicates the actual altitude h in (m), blue line shows the reference signal ETS parameters of the ETS controller: P_k, P_{max}, P_{min} as in (b), (c) *Middle Figure*: The number of fuzzy rules R as the controller evolves, (d) *Bottom Figure*: Rule replacements of the vertical loop ETS control system.

the period of transient time, $P_k > P_{max}$ led to an increase in the number of fuzzy rules from one to four as indicated in Fig. 3b. Meanwhile, Fig. 3c indicates the total number of replacements of fuzzy rules, which took place around 200 times. These computer simulations clearly demonstrate the ability of the ETS control systems to learn from scratch.

B. The Attitude: Pitch Control Loop

The time domain performance of our ETS controller for the longitudinal (pitch) loop is given in Fig 4a. It is clear that our pitch control system works reasonably well considering its reasonably short settling time with minimum overshoots.

Meanwhile, Fig. 4 demonstrates the ability of the ETS controller to adapt to the dynamics of the pitch loop to achieve the desired v_x. Likewise, Fig. 4a denotes how P_k evolves against its upper and lower bounds, while Figs. 4b and 4c highlight the number of fuzzy rules and the number of rule replacements as a part of the self-learning process of the corresponding ETS controller. As with the vertical loop, the

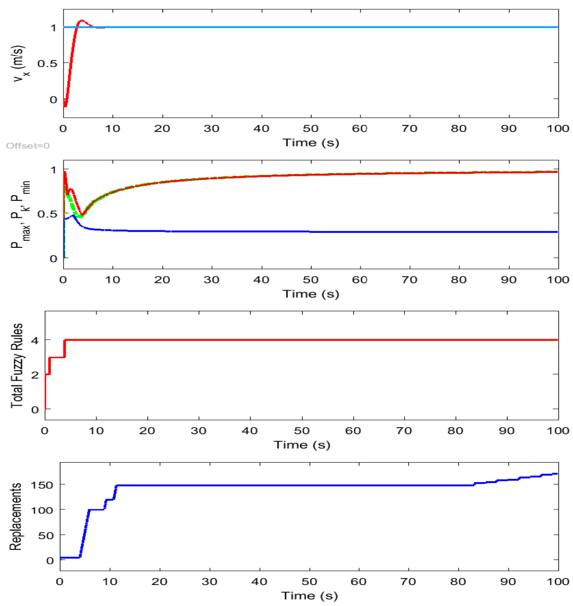

Fig. 4. (a) Step response of the ETS controller in the pitch control loop. The performance of the evolutionary TS-fuzzy controller for the vertical loop for hovering: (b) *Second figure*: The parameters of the ETS controller: P_k, P_{max}, P_{min}, (c) *Third figure*: The number of fuzzy rules R as the system evolves, (d) *Bottom figure*: Rule replacements of the ETS controller.

transient learning period is the moment, where the number of fuzzy rules increases due to the learning process of the system.

VI. Real-Time Experimental Flight Tests

To highlight the efficacy of our fuzzy autopilots, we conducted the real-time flight test experiment using a Tarot hexacopter aerial vehicle. Our indoor flight test facility comprises of 20 VICON motion tracking cameras mounted 4m above the flight test area and encompassing a volume of *9m* × *10m* × *4m*, which was adequate to conduct all of the experiments in this application. The VICON cameras act as a positioning system (fake GPS) to inform our hexacopter about its coordinate positions and orientations. To study the robustness of the closed-loop control systems with respect to severe ground effects, we set a low-altitude reference signal $\bar{z} = 35\ cm$. We will study the efficacy of our fuzzy control systems in their five control loops.

A. The Altitude Control Loop

From Fig. 7, it is clear that our fuzzy autopilot achieved a reasonably good performance as indicated by its reasonably small tracking error signal. Also, the system constantly rejected the ongoing disturbances in the form of hybrid severe *ground effects* and the secondary effects of control due to the constant changes in the attitudes of our hexacopter (pitch and roll). The disturbance rejection capability of the closed-loop fuzzy control system to overcome all these constant disturbances while hovering at low altitudes is our central research focus in this paper. Fig. 7 clearly indicates that our ETS controller can also achieve a reasonably small-steady state hovering error. It should be noted that the figure is much smaller compared to the steady state error of the conventional PID controllers, manually tuned to provide a sufficient damping ratio.

B. The Attitude: Roll Control Loop

The efficacy of the closed-loop fuzzy control system for the trajectory tracking of the roll loop in real-time is given in Fig. 5. The closed-loop roll control system works reasonably

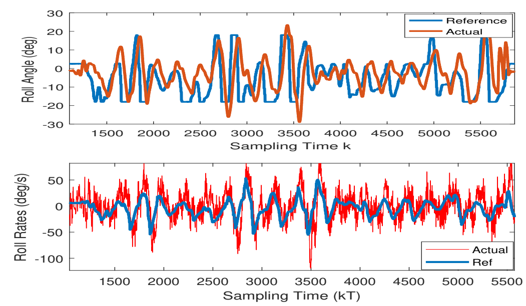

Fig. 5. The real-time trajectory tracking performance of the closed-loop fuzzy control system in the attitude: roll control: (a) Top: the pitch angles, (b) Middle: the control signal of the system to stabilize the pitch loop. Data was taken from the Inertial Measurement Unit (IMU) of our hexacopter aerial vehicle.

well since the actual roll angles were reasonably close to the values of the desired roll angles. While the roll angles are highlighted in the top figure, the fuzzy control signals are indicated in the bottom figure. Overall, the system tracked the reference (command) signal reasonably well in the face of the varying tracking frequencies.

C. The Attitude: Pitch Control Loop

The trajectory tracking performance of the real-time closed-loop fuzzy control system in the pitch loop is given in Fig. 6. Likewise, the closed-loop pitch control system also

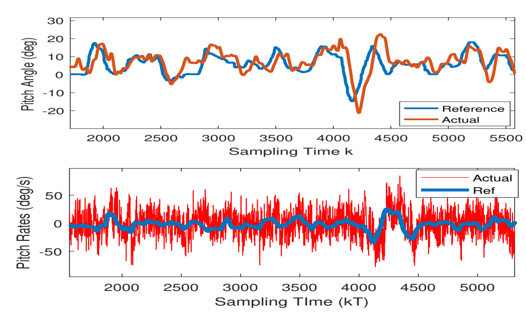

Fig. 6. The real-time trajectory tracking performance of the closed-loop fuzzy control system in the inner loop (pitch) control: (a) Top: pitch angle, (b) Middle: fuzzy control signal to stabilize the pitch loop. Data was taken from the Inertial Measurement Unit (IMU) of our hexacopter.

works substantially well since the actual pitch angles closely track their desired counterparts. The fuzzy control signal is depicted in the bottom figure.

D. The Hovering Performance of the $x - y$ Outer Loop Position Holding Under Severe Ground Effect and Cross-Coupling Disturbance

Furthermore, to highlight the efficacy of the outer loop position controls, namely, the P_x and P_y position control loops; we studied the performance of the systems under a low-altitude hovering condition. As can be seen from Fig. 7, the closed-loop control guided the hexacopter to hover with a substantially small error. The RMSE of the position error along the x-direction was 0.0224 cm, with a mean of $\bar{x} = 0.0114\ cm$ and the standard deviation of $\sigma_x = 0.0194\ cm$ while the RMSE of the position control along the y-axis was 0.1105 cm with $\bar{y} = -0.0386\ cm$ and $\sigma_y = 0.1041\ cm$. This clearly indicates the performance

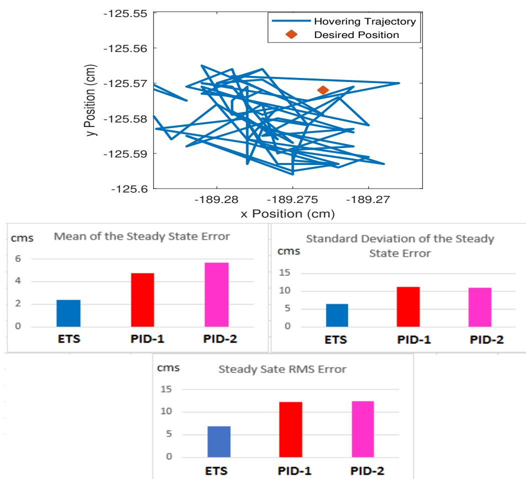

Fig. 7. (a) Top Figure: Real-time high precision of the low-altitude hovering performance with the closed-loop ETS position controllers. (b) Bottom Figure: The *statistical* measures of the steady-state error performance in the altitude loop between our fuzzy control system and the conventional PID controller under severe ground effects and cross-coupling disturbance. For PID-1 the control gains were given by $k_p = 0.000431$, $k_i = 0.00011$, $k_d = 0.0004$ while for PID-2 the control gains were $k_p = 0.000428$, $k_i = 0.00011$, $k_d = 0.00043$.

of our fuzzy autopilot systems to overcome the existing disturbances during low-altitude hovering performance. Bio-inspired optimization algorithms have been widely implemented in machine learning to address the optimal solutions to complex learning problems in the face of large uncertainties. The ETS algorithm mimics the way humans learn by forming the rules required to match the situation (input-output data).

VII. Conclusion

We have shown the capabilities of the evolving TS-fuzzy system to facilitate self-learning in a hexacopter UAV, that is, to perform low-altitude hovering in the face of large uncertainties (e.g. due to ground effects and the secondary effects of control). In addition, we also studied the trajectory tracking performance of the closed-loop control systems. The learning concept in ETS replicates the human ways of learning, that is, to keep and improve some useful and relevant knowledge while forgetting the unused counterparts.

The closed-loop control systems were able to perform online self-learning, eliminating the demand of having *a-priori* knowledge of the fuzzy systems due to online training with incremental fashion performed. Compared to conventional model-based control systems, the ETS controllers are considered more practical in the absence of the requirements of having complex mathematical models, which may not always be available in practice.

References

[1] F. Santoso, M. A. Garratt, and S. G. Anavatti. State-of-the-art intelligent flight control systems in unmanned aerial vehicles. *IEEE Trans. on Automation Science and Engineering*, 15(2):613–627, April 2017.

[2] F. Santoso, M. A. Garratt, S. G. Anavatti, and I. Petersen. Robust hybrid nonlinear control systems for the dynamics of a quadcopter drone. *IEEE Trans. on Systems, Man, and Cybernetics: Systems*, 50(8):3059–3071, 2020.

[3] S. G. Anavatti, F. Santoso, and M. A. Garratt. Progress in adaptive control systems: past, present, and future. In *International Conference on Advanced Mechatronics, Intelligent Manufacture, and Industrial Automation (ICAMIMIA)*, Surabaya, Indonesia, 2015. IEEE.

[4] Y. Zhuang Y. Chen, G. Zhang. Autonomous flight control for multi-rotor UAVs flying at low altitude. *IEEE Access*, 7:42614–42525, 2019.

[5] S Lee, S. H. Kang, and Y. Kim. Trajectory tracking control of quadrotor UAV. In *International Conference on Control, Automation and Systems*, Oct 2011.

[6] P. Pokswa, L. Wang, and A. Mohamed. Gain schedule attitude control of fixed-wing UAV with automatic controller tuning. *IEEE Trans. on Control Systems Technology*, 26(4):1192–1203, July 2018.

[7] D. Leite, R. M. Palhares, V. C. S. Campos, and F. Gomide. Evolving granular fuzzy model-based control of nonlinear dynamic systems. *IEEE Trans. on Fuzzy Systems*, 23(4):923–938, Aug 2015.

[8] K. Sekiguchi. Novel control method for quadcopter-hierarchical linearization approach. In *11th Asian Control Conference (ASCC)*, pages 1853–1858, Gold Coast, QLD, Australia, Dec 2017. IEEE.

[9] J. L. Mendoza-Soto and H. R. Cortes. Generalized predictive control for trajectory tracking of a quadcopter vehicle. In *7 International Conference on Unmanned Aircraft Systems (ICUAS)*, pages 206–212, Miami, FL, USA, USA, July 2017. IEEE.

[10] V. Roberge, M. Tarbouchi, and G. Labonte. Comparison of parallel genetic algorithm and particle swarm optimization for real-time uav path planning. *IEEE Trans. on Industrial Informatics*, 9(1):132–140, Feb 2013.

[11] F. Santoso. A decentralised self-dispatch algorithm for square-grid blanket coverage intrusion detection systems in wireless sensor networks. In *IEEE Vehicular Technology Conference (VTC Fall)*. IEEE, Sept 2011.

[12] F Santoso. Range-only distributed navigation protocol for uniform coverage in wireless sensor networks. *IET Wireless Sensor Systems*, 5(1):20–30, Dec 2014.

[13] D. Howard. A platform that directly evolves multirotor controllers. *IEEE Trans. on Evolutionary Computation*, 21(6):943–955, Dec 2017.

[14] X. Liu, Y Liu, Y. Chen, and L. Hanzo. Trajectory design and power control for multi-uav assisted wireless networks: A machine learning approach. *IEEE Trans. on Vehicular Technology*, 68(8), 2019.

[15] F. Santoso, M. A. Garratt, and S. G. Anavatti. Fuzzy logic-based self-tuning autopilots for trajectory tracking of a low-cost quadcopter: A comparative study. In *International Conference on Advanced Mechatronics, Intelligent Manufacture, and Industrial Automation*, pages 64–69, 2015.

[16] A. Alaimo, V. Artale, C. Milazzo, A. Ricciardello, and L. Trefiletti. Mathematical modeling and control of a hexacopter. In *International Conference on Unmanned Aircraft Systems (ICUAS)*, pages 1043–1050, Atlanta, May 2013.

[17] M. Moussid, A. Sayouti, and H. Medromi. Dynamic modeling and control of a hexarotor using linear and nonlinear methods. *International Journal of Applied Information Systems*, 9(5):9–17, Aug 2015.

[18] R.C. Nelson. *Flight Stability and Automatic Control*, volume 2. McGraw-Hill, 1998.

[19] J. M. Seddon and S. Newman. *Basic Helicopter Aerodynamics*. Wiley, June 2011.

[20] M. Garratt and S. Anavatti. Non-linear control of heave for an unmanned helicopter using neural network. *Journal of Intelligent and Robotic Systems*, 66(4):495–504, June 2012.

[21] P. Angelov and D. P. Filev. An approach to online identification of takagi-sugeno fuzzy models. *IEEE Trans. on System, Man, and Cybernetics - Part B: Cybernetics*, 34(1):484–498, Feb 2004.